Rotational Reorientation Dynamics of Oxazine 750 in Polar Solvents

Panwang Zhou,[†,‡] Peng Song,[†,‡] Jianyong Liu,[†] Ying Shi,[†] Keli Han,*[,†] and Guozhong He[†]

State Key Laboratory of Molecular Reaction Dynamics, Dalian Institute of Chemical Physics, Chinese Academy of Science, Dalian 116023, Liaoning, China, and Graduate School of Chinese Academy of Sciences, Beijing 100049, China

Received: December 26, 2007; In Final Form: January 29, 2008

The rotational reorientation dynamics of oxazine 750 (OX750) in the first (with pump pulse at 660 nm) and a higher excited state (with pump pulse at 400 nm) in different polar solvents have been investigated using femtosecond time-resolved stimulated emission pumping fluorescence depletion (FS TR SEP FD) spectroscopy. In both excited states, three different anisotropy decay laws have been observed for OX750 in different solvents. Only in acetone and formamide could the anisotropy decays of OX750 be described by single-exponential functions, whereas the anisotropy decays have been found to exhibit biexponential behavior in other solvents. The slower anisotropy decay observed in all of the solvents has been assigned to the overall rotational relaxation of OX750 molecules, and a quantitative analysis of this time constant has been performed using the Stokes−Einstein−Debye hydrodynamic theory and the extended charge distribution model developed by Alavi and Waldeck. In both methanol and ethanol, a faster anisotropy decay on the order of picoseconds and a slower anisotropy decay on the hundreds of picoseconds time scale are observed. The most likely explanation for the faster anisotropy involves the rotation of the transition dipole moment in the excited state of OX750 resulting from the electron transfer (ET) reaction taking place from the alcoholic solvents to the OX750 chromophore. As a possible explanation, the wobbling-in-the-cone model has been used to analyze the biexponential anisotropy decays of OX750 in dimethylformamide (DMF) and dimethyl sulfoxide (DMSO). The observed faster anisotropy decays on the hundreds of femtoseconds time scale in DMF and DMSO are ascribed to the wobbling-in-the-cone motion of the ethyl group of OX750, which is sensitive to the strength of the hydrogen bond formed between the solvent and the protonation site of OX750.

Introduction

The experimental and theoretical studies of molecular rotational relaxation in solutions have been an area of interest in recent years and have been used extensively to elucidate the fundamental nature of solvent−solute interactions.[1−3] When a molecular system is excited by an intense, polarized, and ultrashort pulse of light, the equilibrium distribution of molecular orientations can be disturbed (a hole is burned in the orientational distribution), and the orientational hole may be filled by ultrafast rotational motion, electronic relaxation, or energy transfer.[3] In recent years, the development of pico- and femtosecond lasers has allowed researchers to directly probe these ultrafast relaxation processes in solutions by time-resolved fluorescence or absorption depolarization spectroscopy. In addition, several novel methods, including IR/UV double-resonance spectroscopy,[4−5] 2D IR vibrational spectroscopy,[6] femtosecond three-pulse transient anisotropy,[7] have been developed to study these relaxation processes.

The Stokes−Einstein−Debye (SED) hydrodynamic theory[1] is an early treatment of molecular rotational motion in liquids. In this diffusion-based theory, the solute molecule is modeled as a hard sphere and the solvent as a continuum. It has been extended to symmetric and asymmetric ellipsoidal solute shapes. According to the SED theory, the reorientation time of a solute in a solvent continuum is proportional to its volume, the solvent viscosity and inversely proportional to the temperature. A large number of experimental investigations have been carried out to check the validity and applicability of the SED model.[8−28] The results have shown that the SED theory works well when the coupling between the solute and the solvent is purely mechanical or hydrodynamic in nature. This is suitable for conditions in which either the solute or the solvent is nonpolar, or both of them are nonpolar. However, the deviations are generally observed between the experimentally measured reorientation times and the calculated ones using the SED theory when the solute and solvent are both polar in nature. The observed deviations result from two causes: one is the specific interactions between solute and solvent like hydrogen bonding,[3,23−25] the other is the electrical aspects of solute−solvent coupling, known as the dielectric friction.[13−18,26−28] Apart from the above-mentioned effects, the reorientation time of the solute in solutions is also affected by the size of solute with respect to the size of solvent.[29,30]

When the orientational relaxation is studied with time-resolved fluorescence spectroscopy, the molecule is first excited by a polarized light; then the intensities of fluorescence polarized in planes parallel ($I_{||}(t)$) with and perpendicular ($I_{\perp}(t)$) to the polarization plane of the exciting light, as a function of the time following the excitation, can be measured. The polarization anisotropy function is given by the following expression:

$$r(t) \equiv \frac{I_{||}(t) - I_{\perp}(t)}{I_{||}(t) + 2I_{\perp}(t)} \quad (1)$$

* Corresponding author. E-mail: klhan@dipc.ac.cn.
† Dalian Institute of Chemical Physics, Chinese Academy of Science.
‡ Graduate School of Chinese Academy of Sciences.

10.1021/jp7120998 CCC: $40.75
Published on Web 03/26/2008

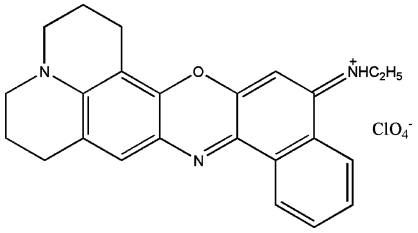

Figure 1. Structural formulas of oxazine 750.

It is well-known that, when the solute molecule is modeled as an asymmetric ellipsoid and the transition moment directions for excitation and the emission are the same, the $r(t)$ function contains at the most five exponentials.[1,31,32] However, in practice, for the vast majority of probes, only single exponential anisotropy decays have been observed. (The sole exception is highly symmetric and rigid molecule such as anthracene,[4,5,33,34] for which the biexponential anisotropy decay is observed.) The reason is that the difference in magnitude between the correlation times of the solute molecules along the different axes of rotation is not significant; hence, the measured reorientation time represents the average of the correlation times.[24] Although this is common for most experimental investigations, the exceptions have also been observed by few of authors. Recently, Horng et al.[35] studied the rotational dynamics of coumarin 153 (C153, an asymmetric molecule) in a number of solvents and the biexponential anisotropy decays for C153 were found in some polar solvents. Horng and colleagues[35] ascribed such biexponential anisotropy decay to the effects of non-Markovian friction on the rotational motion. Using the optically heterodyned polarization spectroscopy method, Sukharevsky et al.[36] measured the orientational anisotropy of a host−guest bimolecular complex. In addition to a long time of anisotropy decay for the complex (which was assigned to the overall orientational relaxation of the complex), a short time of anisotropy decay also was observed, which was ascribed to the relative internal motion of chromophore with respect to the host molecule. Studying the microscopic inhomogeneity and ultrafast orientational motion in an organic photovoltaic bulk heterojunction thin film by 2D IR vibrational spectroscopy, Barbour et al.[6] found that the butyric acid methyl ester group of 6,6-phenyl-C_{61}-butyric acid methyl ester (PCBM) undergoes ultrafast wobbling-in-the-cone orientational motion on the 110 fs time scale within a cone semiangle of 29°, and following this motion, the PCBM molecules then undergo diffusive orientational motion on the 22 ps time scale. It is noteworthy that all of the fast anisotropy decays observed in the above-mentioned works occurred in order of femtosecond to subpicosecond. As most previous studies of rotational relaxation of probes in solvent have involved picosecond time-resolved spectroscopy, it is meaningful to extend the time scale to femtosecond. This will help provide a complete understanding of the rotational reorientation dynamic and a deeper insight into the mechanisms of the rotational relaxation process.

The femtosecond time-resolved stimulated emission pumping fluorescence depletion (FS TR SEP FD) technique has been used to study vibrational relaxation and solvation dynamics of organic molecules[37−41,43−45] and the fast internal conversion of the chlorophyll a from higher electronically excited states.[42] In this study, we used FS TR SEP FD spectroscopy to investigate the rotational dynamics of oxazine 750 (OX750) (see Figure 1) in protic and aprotic polar solvents, such as methanol, ethanol, acetone, dimethyl sulfoxide (DMSO), dimethylformamide (DMF), and formamide. The nonexponential anisotropy decays for OX750 were observed in most of solvents being investigated, with the exceptions of acetone and formamide, for reasons that will be elucidated in the results and discussion section. The contribution from the hydrodynamic friction to the reorientation time was calculated using the SED theory. Because of the polar molecular structure of OX750 and the fact that it ionizes when dissolved in solution, the contribution from dielectric friction was calculated using the extended charge distribution model developed by Alavi and Waldeck.[46,47]

Experimental Section

The solute OX750 used in the present study was purchased from Exciton as perchlorate and dissolved in solvents with a concentration of 8×10^{-4} M. The rotational reorientation time of OX750 in different solvents was measured using the FS TR SEP FD technique. The details of the experimental setup have been described in elsewhere,[42,43] so only a brief description is given here.

The Spectra-Physics Hurricane system was used as the laser source. This system comprises a seeded laser (Mai Tai, cw diode-pumped laser and a mode-locked Ti sapphire pulse laser), a pump laser (Evolution, diode-pumped Q-switched Nd:YLF laser), a stretcher, a Ti sapphire regenerative amplifier, and a compressor. The output power of the system was about 500 mW at 1 kHz repetition rate at 800 nm with a pulse width of <130 fs (FWHW). The pulses from the amplifier were used to pump an optical parametric amplifier (OPA). In the experiments, the 400 and 660 nm pulses were used to excite the sample to generate fluorescence and the spared laser (800 nm) from the OPA as a probe pulse. The 400 nm pulses were generated by frequency doubling with a BBO crystal (0.3 mm β-BaB_2O_4, Fujian Castech Crystals Inc.) and the 660 nm pulses from the OPA. The probe beam is collinear with the pump beam, both of which were focused. The fused quartz sample cell was placed in a spot behind the focus at which the beam diameter was 2 mm to avoid the thermal effect of the sample due to the laser heating. The optical path of the probe beam was altered by a motorized translational stage (Unidex-100, Aerotech Inc.) using computer technology, providing 2×1 μm path difference increments, equivalent to 6.67 fs. The polarization of probe beam with respect to the polarization of pump beam was adjusted to 0° for the parallel component ($I_{\parallel}(t)$) and to 90° for the perpendicular component ($I_{\perp}(t)$), with a half-wave plate placed in the path of probe beam. The intensity of fluorescence (720 nm) perpendicular to the incident beams was focused into a monochromator (WDG30, Beijing Optical Instrument Factory) and detected by a photomultiplier tube (R456, Hamamatsh Corp.). The signal was processed by a Boxcar (SR250, Stanford Research Systems, USA), and electronically recorded. The polarization anisotropy function was calculated using eq 1. The cross-correlation function was determined according to the 1 + 1′ two-photon fluorescence methods described in refs 37−39, in which the time resolution was estimated to be ∼230 fs and without further optimization. All fluorescence depletion signals were measured at room temperature. Multiple time-step scans were used in data collection. The calculated anisotropy decays were fitted to the exponentials function using a nonlinear least-squares algorithm without deconvolution.

Steady-state absorption and emission spectra of the OX750 in all tested solvents were measured with a UV−visible absorption spectrophotometer (HP8453, Hewlett-Packard Corp.) and a spectrofluorometer (C-700, Photo Technology International Corp.), respectively.

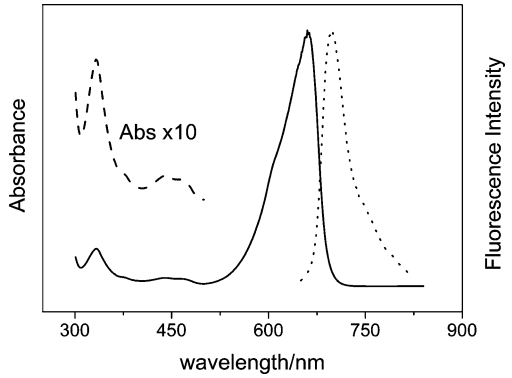

Figure 2. Steady-state absorption (solid) and fluorescence (dot) spectra of oxazine 750 in methanol.

Computational Methods

Ab initio molecular orbital methods were used to investigate the structure and charge distributions of OX750 in gas phase. The ground-state geometry was fully optimized (without any symmetry constraint) using the B3LYP hybrid density functional,[48−50] which is well-know to yield accurate ground-state geometries. The 6-311+G** basis set was used for optimization. From the ground-state geometry, vertically excited singlet-state calculation was performed using the time-dependent density functional method (TD-DFT) with the same basis set. To optimize the geometry of the first excited single state, the single-excitation configuration-interaction (CIS) method with the 6-311G* basis set was used to perform the vertically excited singlet-state calculation. All the calculations in this work were carried out with the Gaussian 03 electronic structure program.[51] Partial atomic charges for the first excited singlet state were calculated using the Mulliken population analysis scheme as implemented in the Gaussian package.

Results and Discussion

First, to determine the wavelength of the pump and probe pulse, the steady-state spectra of OX750 have been measured in all the solvents used here, although some of them have been reported earlier.[55,56] The typical steady-state absorption and fluorescence spectra of OX750 in methanol are shown in Figure 2. Other spectra data are shown in Table 1. The absorption maximum of the S_1 band of OX750 is at 660 nm and the emission maximum is at 699 nm in methanol. From Table 1, it can be seen that the absorption and emission positions are less dependent on the solvents. Thus, the OX750 molecules will be excited from the ground state to the lowest excited state (S_1) and a higher excited state (S_n) with the pump pulse at 660 and 400 nm, respectively.

The measured reorientation times of OX750 in different solvents with the pump pulse at 660 and 400 nm are presented in Table 2. It is found that the experimentally measured anisotropy decays of OX750 in different solvents can be divided into three groups: acetone and formamide, methanol and ethanol, DMF and DMSO. In acetone and formamide, the experimentally measured anisotropy decays can be adequately described by single-exponential functions. The best fitted relaxation time was 51 (57) ps for acetone and 362 (363) ps for formamide with the pump pulse at 660 (400) nm. In DMF and DSMO, the anisotropy decays of OX750 molecules have been found to exhibit biexponential behavior, and the double exponential functions have been used to fit the experimentally measured data. The best fit parameters for the biexponential

TABLE 1: Steady-State Absorption and Fluorescence Spectra of Oxazine 750 in Various Solvents

	methanol	ethanol	Acetone	DMF	DMSO	formamide
absorption λ_{ab} (nm)	660	666	664	671	672	671
emission λ_{em} (nm)	699	703	703	693	712	703

form are a subpicosecond component and a hundreds of picoseconds component. Representative time-resolved decays of OX750 in acetone and DMF with the pump pulse at 660 nm are shown in Figure 3. The different anisotropy decay laws of OX750 in acetone and DMF can be seen clearly from Figure 3. In methanol and ethanol, both the single and double exponential functions can be used to fit the experimentally measured data. Figure 4 shows the measured anisotropy decays and simulated results for OX750 in ethanol with the pump pulse at 660 nm, where the data are plotted on a logarithmic time axis. This method of presenting the data makes the deviations of the fitted curve from the measured data more apparent. The single and double exponential fits are shown by the dashed and solid line, respectively. It is apparent from the plot that the double-exponential decay law provides much better agreement with the data. A comparison of the reduced χ^2 values for the two fits shows that the reduced χ^2 value for the double exponential is about 4 times smaller than that for the single exponential. The residuals for single exponential (top panel) and double exponential (middle panel) fits are also shown in Figure 4. From the plots it can be seen that the residuals for double exponential are smaller and more random than those for the single exponential. All results confirm that a second component is actually present in the anisotropy decay, and its contribution cannot be regarded as negligible. However, the fitted fast time constants for OX750 in methanol and ethanol are much longer than those in DMF and DMSO (see Table 2). This may indicate that the nonexponential anisotropy decay laws for OX750 in alcoholic (methanol and ethanol) and aprotic polar solvents (DMF and DMSO) result from different sources.

The long time anisotropy decays observed in all the solvents can be safely assigned to the overall rotational relaxation of the OX750 molecules, and a quantitative analysis is presented in the following two subsections. The assignment of the short time anisotropy decays observed in other solvents should be considered carefully, and detailed discussions are presented in the third subsection. From Table 2 it can be seen that the experimentally measured anisotropy decay law of OX750 on the pump pulse at 400 nm is similar to that on the pump pulse at 660 nm, and the discussions in the following three subsections thus are focused on the anisotropy decays on the pump pulse at 660 nm. The final subsection will discuss the anisotropy decays on the pump pulse at 400 nm.

A. Mechanical Friction. To analyze the experimental observations, the Stokes−Einstein−Debye (SED) hydrodynamic theory has been employed as a preliminary step. According to the SED theory, when the solute molecule is modeled as an asymmetric ellipsoid and the transition moment directions for both excitation and the emission are identical, the full expression for the orientation correlation function $r(t)$ (taken from ref 1) is

$$\frac{5}{6}r(t) = \sum_{i=1}^{3} c_i \exp(-t/\tau_i) + \left(\frac{F+G}{4}\right)\exp(-(6D-2\Delta)t) + \left(\frac{F-G}{4}\right)\exp(-(6D+2\Delta)t) \quad (2)$$

TABLE 2: Rational Reorientation Time of Oxazine 750 in Various Solvents with Pump Pulse at 660 and 440 nm, Together with Viscous and Dielectric Properties of the Solvents

				660 nm		400 nm	
solvent	η (mPa·s)	ϵ	τ_D/ps	τ_1/ps	τ_2/ps	τ_1/ps	τ_2/ps
acetone	0.316	20.56[a]	4[b]		50.6 ± 0.3		57.1 ± 0.8
methanol	0.553	33.7[c]	55.6[c]	12.3 ± 2.2	108.8 ± 2.8	18.6 ± 2.3	142.6 ± 3.9
ethanol	1.06	24.3[c]	139[c]	18.6 ± 2.7	226.0 ± 12.0	27.4 ± 4.3	215.4 ± 10.8
DMF	0.802	36.7[c]	10[c]	0.255 ± 0.023	136.7 ± 2.7	0.475 ± 0.05	142.6 ± 2.8
DMSO	1.996	46.5[c]	20.6[c]	0.346 ± 0.03	263.2 ± 7.0	0.748 ± 0.098	248.6 ± 9.6
formamide	3.302	108.2[c]	39[c]		362.3 ± 12.7		362.8 ± 17.5

[a] From ref 52. [b] From ref 53. [c] From ref 54.

where $c_i = \alpha_k^2\alpha_j^2$ and $i \neq j \neq k$. The α_i's are the direction cosines of the absorption dipole with respect to the long axis of the molecule. The time constants τ_i are

$$\tau_i = \frac{1}{3D + 3D_i} \tag{3}$$

where D_i is the diffusion coefficient for rotation about axis i and D is the mean-diffusion coefficient defined as

$$D = \frac{D_1 + D_2 + D_3}{3} \tag{4}$$

The other terms in eq 2 are defined as

$$F = \sum_{i=1}^{3} \alpha_i^4 - \frac{1}{3} \qquad G\Delta = \sum_{i=1}^{3} D_i(\alpha_i^4 + 2\alpha_j^2\alpha_k^2) - D \tag{5}$$

and

$$\Delta = \sqrt{D_i^2 + D_j^2 + D_k^2 - D_iD_j - D_jD_k - D_kD_i} \tag{6}$$

Integrating the eq 2 over all time yields the following expression for the reorientation time:[20,57]

$$\tau_r = \frac{6}{5r_0}\left(c_1\tau_1 + c_2\tau_2 + c_3\tau_3 + \frac{F+G}{4(6D-2\Delta)} + \frac{F-G}{4(6D+2\Delta)}\right) \tag{7}$$

If the transition dipole is along the long axis of the molecule, eq 8 reduces to

$$\tau_r = \frac{6}{5r_0}\left(\frac{F+G}{4(6D-2\Delta)} + \frac{F-G}{4(6D+2\Delta)}\right) \tag{8}$$

The diffusion coefficient about axis i is given by[1,57]

$$D_i = \frac{kT}{\zeta_i} \tag{9}$$

where k is the Boltzmann constant, T is the absolute temperature, and ζ_i is the friction coefficient about axis i. As discussed earlier, in addition to the mechanical (ζ_{mech}) or hydrodynamic friction, a polar molecule rotating in a polar solvent also experiences hindrance due to dielectric friction (ζ_{diel}). In general, long-range electrostatic forces do not simply add an independent contribution to the friction due to short-range or mechanical sources because the electro-hydrodynamic coupling exists between the two contributions to the friction.[58−62] However, in practice, as a useful approximation, the total friction ζ_{total} experienced by the solute molecule can be written as the sum of mechanicaland dielectricfrictions in the absence of a theory that completely bypasses the division of the total friction into two separable components. Thus, the ζ_{total} is calculated using the relation

$$\zeta_{total} = \zeta_{mech} + \zeta_{diel} \tag{10}$$

This practice has been followed in literature[13−18, 26−28, 57] in the past few decades. In this subsection, only the mechanical friction is considered and calculated. The dielectric friction will be calculated and discussed in the following subsection. It is well-known that, in the hydrodynamic model, the two extremes for the boundary conditions are referred to as "slip" for weak coupling and "stick" for strong coupling. The mechanical friction is given by the relation

$$\zeta_{mech} = 6V\sigma_{SLIP}\eta \tag{11}$$

for the slip boundary condition and

$$\zeta_{mech} = V\sigma_{STICK}\eta \tag{12}$$

for the stick boundary condition, where V is the molecular volume and η is the solvent's shear viscosity. The parameters σ_{SLIP} and σ_{SLICK} account for the nonsphericity of the solute along with the slip and stick boundary condition, respectively.

The ground-state geometry of OX750 was obtained by performing an ab initio calculation at the B3LYP/6-311+G** level. From this geometry, the axial radii of the molecule is estimated to be 7.6:5.5:1.9 Å. The van der Waals volume of OX750 was estimated to be 334 Å^3 using Edward's increment method.[63] The σ_{SLIP}'s along three axes were obtained by interpolating the numerical tabulations of Sension and Hochstrasser,[64] whereas the σ_{STICK}'s were obtained from the numerical tabulations of Small and Isenberg.[65] Using the obtained parameters, the friction coefficients ζ_i's along the three principal axes of rotation were calculated, and the diffusion coefficients D_i's were obtained using eq 10. According to the result of TD-DFT calculation as described in computational section, the projections of transition dipole from the ground state to the first excited state along with three axes were estimated to be 9.21, 0.12, and −0.13 Debye, respectively. This indicates that the transition dipole moment is almost along with the long axis. From these obtained parameters, the reorientation times of OX750 now can be calculated using eq 8.

Figure 5 shows the experimentally measured reorientation times of OX750 and the calculated slip and stick lines using the SED theory. From Figure 5, it can be seen that, in the alcoholic solvents (methanol and ethanol), the experimentally measured reorientation times are larger than the stick limits. However, in the aprotic solvents and formamide, the experimentally measured reorientation times are matched with or smaller than the stick limits. It has been well documented that the rotation of an ionic solute in a polar solvent should follow stick boundary condition.[20,28,53,54,66−68] However, according to the analysis below, this may not be the case for OX750. First,

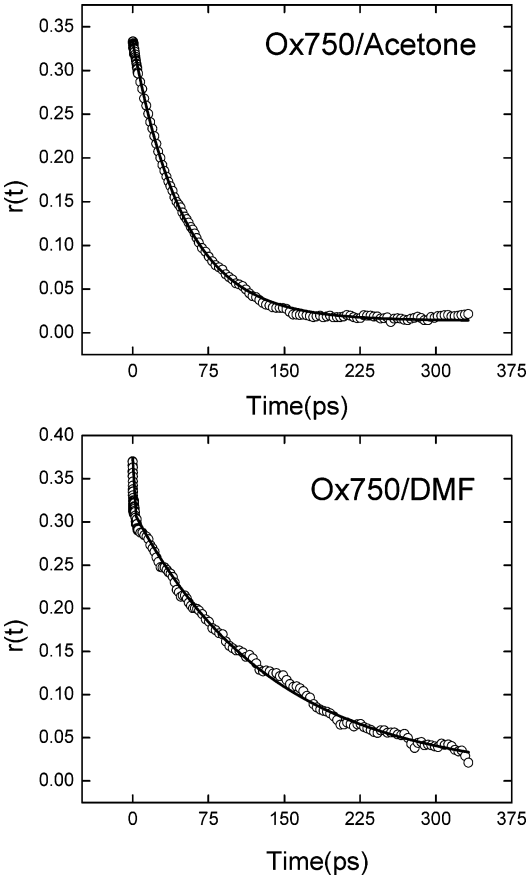

Figure 3. Anisotropy decays for oxazine 750 in acetone (top) and DMF (bottom): (○) experimental data; (—) simulated results. In the top panel, the solid line is a best fit to a single exponential, and in the bottom panel, it is a best fit to a double exponential.

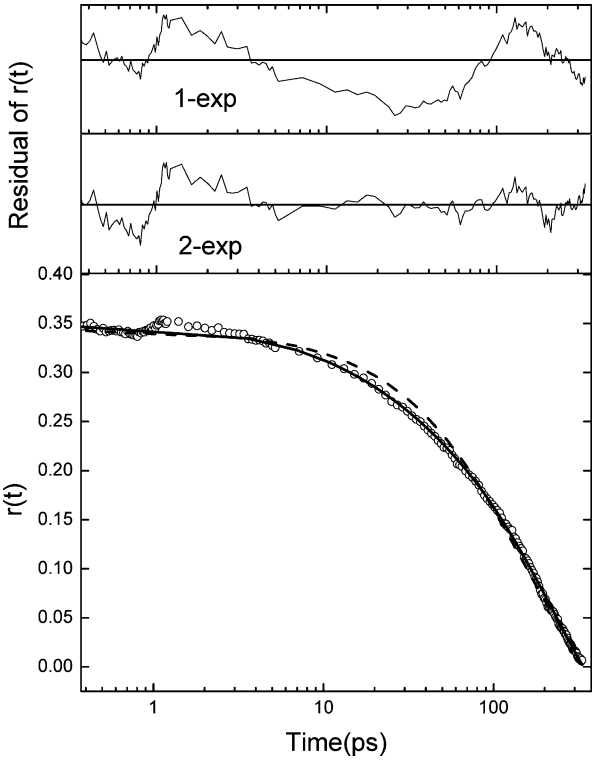

Figure 4. Anisotropy decay of oxazine 750 in ethanol, which can be fitted by single-exponential and biexponential functions. The data are plotted on a logarithmic time axis. The hollow circles shown in the bottom panel are the experimental data. The dashed line represents the single-exponential fit to the $r(t)$ data, and the solid line represents the biexponential fit to the $r(t)$ data. The two top panels are the residuals of single-exponential (top) and biexponential (middle panel) fits.

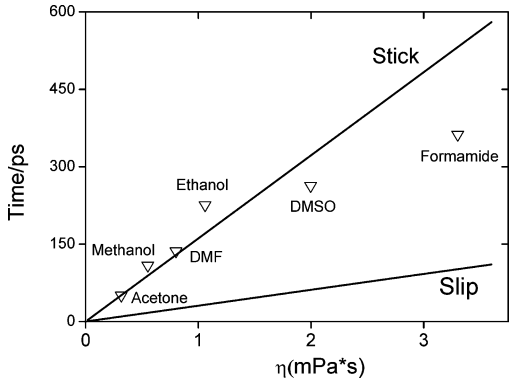

Figure 5. Experimentally measured τ_r (▽) vs η for oxazine 750 in solvents. The slip and stick lines calculated using the SED theory are also shown.

as a polar and ionic molecule, OX750 will experience hindrance due to dielectric friction besides the hydrodynamic friction, because it is dissolved in polar solvents in current work. Second, all of the solvents used in the present study can form a hydrogen bond with the protonation site of OX750. In addition, another hydrogen bond can be formed between the nitrogen atom in the central ring of OX750 and the protic solvent (methanol, ethanol, and formamide). As mentioned in the Introduction, both of these effects can make the measured reorientation time longer than that predicted by the SED theory. In a recent series of papers, Dutt et al. have studied the rotational dynamics of two structurally similar nondipolar probes in hydrogen bonding solvents (ref 3 and references therein). The probe, 1,4-dioxo-3,6-diphenylpyrrolo[3,4-*c*]pyrrole (DPP) with two NH groups, was found to rotate 2−3 times slower than its dimethyl counterpart, 2,5-dimethyl-1,4-dioxo-3,6-diphenylpyrrolo[3,4-*c*]-pyrrole (DMDPP) in which two N−CH_3 groups replace the two NH groups. This demonstrates that the hydrogen bond between the solute−solvent actually hinders the molecular rotation. Thus, it is not surprising that the reorientation times of OX750 in methanol and ethanol are larger than the stick limits, as an additional hydrogen bond was formed between the OX750 and these solvents as compared with the aprotic solvents. However, it is still surprising that the OX750 displays a very fast reorientation time in formamide and experiences it rather as an aprotic solvent. It should be noted here that the obtained reorientation time for OX750 in formamide is not accurate, because of the limited scan range of the FS TR SEP FD instrument. At the end time of our scan range (350ps), the value of the anisotropy for OX750 in formamide decayed only to about 0.15 and did not tend toward a constant, indicating that the complete anisotropy decay is not obtained for OX750 in formamide. Thus, further discussion on this reorientation time may not be meaningful. According to the above discussions, the slip boundary condition may be more appropriate for OX750, because the experimentally measured reorientation times in aprotic solvents are not greater than the stick limits. The differences between the measured reorientation times and the calculated ones using the SED theory with the slip boundary condition account for the special solute−solvent interactions.

Although there are no reported reorientation times for OX750 in earlier publications, the rotational dynamics of several molecules, which have structures similar to those of OX750, such as nile blue A (NB),[53,54,66,67] oxazine 720,[53,54,66,67] and cationic forms of neutral red,[20,28] have been studied. The

experiment results show that, even in the aprotic solvents, the measured reorientation times are apparently larger than the stick limits. Thus, the stick boundary condition has been used by these authors to interpret the rotational dynamics results for the above-mentioned cationic molecules. Recently, Kurnikova et al.[68] studied the rotational relaxation of three structurally similar solutes: resorufin (anion), resorufamine (neutral), and thionine (cation) in DMSO, using molecular dynamics (MD) studies and polarization spectroscopy. The experiment results show that the anion exhibits a fast, nearly "slip" rotational relaxation; the resorufamine (neutral) relaxation is twice as slow, which puts it between the "slip" and "stick" regimes; and the cation relaxes even more slowly than those two, and the reorientation time is longer than that predicted by stick limit: it is in the "superstick" regime. In spite of having similar shapes and sizes, these three solute molecules experience identical mechanical or hydrodynamic friction. From dielectric friction calculations, it was shown that the dielectric friction levels are also similar for the three probes. MD studies have demonstrated that the differences arise mainly from changes in the solute's ability to associate with DMSO molecules.[68] The slowest molecule, cation (thionine), offered two association sites (amino groups) for the DMSO and was able to attract as many as four DMSO molecules simultaneously. Neutral solute (resorufamine) appears to form a stable complex with only one DMSO at a time and the anion (resorufin) cannot form any stable solute−solvent complex on the time scale of rotational dynamics. Kurnikova and colleagues argued that the charge on the probe molecule determines whether a solute can form a stable complex with the solvent.[68] However, it must be noted that thionine, resorufamine, and resorufin have two, one, and zero amino groups, respectively. Thus, a later study by Dutt et al.[28] have demonstrated that it is the nature of the functional group rather than the charge that plays an important role in determining the additional friction experienced by the solute molecule. They have studied the rotational relaxation of cationic and neutral forms of the same solute, red neutral in DMSO.[28] Their results show that the cationic form of neutral red rotates marginally slower (less than 20%) than the neutral form in DMSO.[28] The reason for the observed slower rotation of the cationic form has been ascribed to the extra hydrogen atom attached to the ring nitrogen, which can serve as an additional site for the association of the DMSO molecule. Comparing the structures of NB, oxazine 720, and the cationic forms of neutral red with the OX750, it can be observed that both the NB and oxazine 720 have two NH groups, the cationic forms of neutral red has one NH_2 and one NH group, whereas OX750 has only one NH group. That is to say, in the aprotic solvents that can form hydrogen bonds with the NH group, these molecules can associate with more solvent molecules than OX750, thus causing a longer reorientation time for these molecules compared with OX750. Because all the aprotic solvents used in previous studies[20,28,53,54,66,67] and in current work can associate with the NH group, it is not surprising that the reorientation times of these molecules in the aprotic solvents are in the "superstick" regime, whereas the OX750 is followed between the slip and stick limits.

B. Dielectric Friction. There are at least three models that can be used to calculate the dielectric friction: the semiempirical model proposed by van der Zwan and Hynes (ZH),[69] the continuum theories of Nee-Zwanzig (NZ),[70] and the extended charge distribution model developed by Alavi and Waldeck (AW).[46,47] In the ZH model the fluorescence Stokes shift of the solute in a given solvent is related to the dielectric friction. Whereas the NZ model treats the solute as a point dipole rotating in a spherical cavity, the AW model is an extension of NZ theory, in which the solute is treated as a distribution of charges instead of a point dipole and the dielectric friction arises from the torque generated between the solute field and the reaction field in the solvent. In our analysis, the AW model is used to calculate the dielectric friction because previous studies have shown that this model reproduces experimental reorientation times more closely than do the point dipole models.[13−17,46,57,60] According to the AW model, the dielectric friction is given by[46,47]

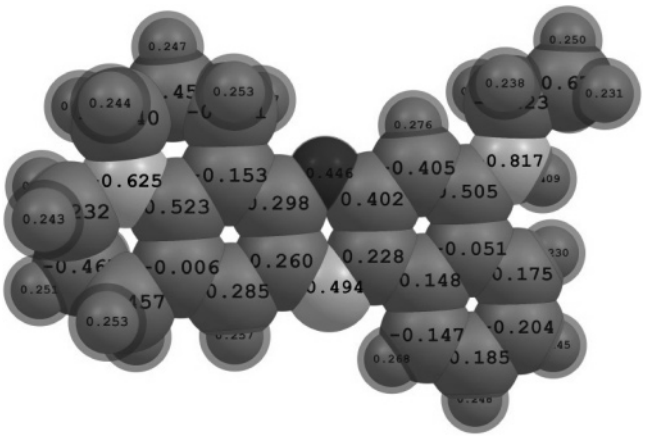

Figure 6. van der Waals surface of oxazine 750 with the partial atomic charge distributions used in the analysis.

$$\zeta_{\text{diel}} = \frac{8(\epsilon_0 - 1)}{a(2\epsilon_0 + 1)^2}\tau_D \sum_{j=1}^{N}\sum_{i=1}^{N}\sum_{L=1}^{L_{\max}}\sum_{M=1}^{L} \times \left(\frac{2L+1}{L+1}\right)\frac{(L-M)!}{(L+M)!} M^2 q_i q_j \left(\frac{r_i}{a}\right)^L \left(\frac{r_j}{a}\right)^L P_L^M(\cos\theta_i)\, P_L^M(\cos\theta_j)\cos M\phi_{ij} \quad (13)$$

where $P_L^M(x)$ are the associated Legendre polynomials, a is cavity radius, N is the number of partial charges, and q_i is the partial charge on atom i, whose position is given by (r_i, θ_i, ϕ_i), and $\phi_{ij} = \phi_i - \phi_j$. The parameters ϵ_0 and τ_D are the zero-frequency dielectric constant and the Debye relaxation time of the solvent, respectively. The value of parameter L describes the spatial variation of the charge distribution at the cavity surface.[16] $L_{\max}$ is the cutoff value of L above which the solvent cannot respond to the charge variation at the cavity surface as the solute reorients. In the nonassociative solvents, such as DMSO and DMF, the value of $L_{\max}$ can be chosen by computing the number of solvent molecules that can be packed on the surface of the cavity.[22,27] Hence, the value of $L_{\max}$ depends on the relative size of the solute and the solvent, and can be calculated using the formula[16]

$$L_{\max} = 2\frac{(r_{\text{solute}} + r_{\text{solvent}})^2}{(r_{\text{solvent}})^2} \quad (14)$$

where r_{solvent} and r_{solute} are the radii of the solvent and the solute, respectively.

The excited-state charge distribution of OX750 was presented in Figure 6. The long axial radius was taken as r_{solute} for OX750, which is 7.6 Å. The r_{solvent} for acetone, DMF, and DMSO were obtained from the van der Waals volume of the solvents and

treated as spheres, which are 2.49, 2.65, and 2.64 Å, respectively. The L_{max} values obtained for OX750/acetone, OX750/DMF, and OX750/DMSO using eq 14 are 33, 30, and 30, respectively. The friction calculated from the AW model is very sensitive to the cavity radius chosen for the molecule, and this sensitivity results from the placement of charge near the cavity boundary.[46] Thus, in practice, the value of cavity radius is used as an adjustable parameter, and this approach has been used by several authors.[16,22,27,71,72] The best fit cavity radius should be closer to the long axial radius of the solute molecule or, within a set of solutes with similar dimensions the consistency of best fit cavity radius should be achieved.[71] Friction coefficients about each axis were calculated by summing the mechanical and the dielectric friction according to eq 10. The diffusion coefficients that result from using eq 9 were then used to calculate the reorientation times using eq 8, which assumes that the transition dipole moment is along with the long axis.

The best fit cavity radii for OX750/acetone, OX750/DMF, and OX750/DMSO are 9.23, 8.85, and 8.83 Å, respectively. With these values of cavity radii, the experimentally measured reorientation times can be accurately reproduced by the theoretical model. The agreement between theory and experiment is within 1%. In DMF and DMSO, the values of best fit cavity radii are almost the same and about 16% longer than the long axial radius of OX750. In acetone, the value of best fit cavity radius is longer than that in DMF and DMSO and is about 21% longer than the long axial radius of OX750. The differences between the best-fit radii and the long axial radius are quite reasonable, considering that the size of solute with respect to the size of solvent is not included in our analysis. For associative solvents, typically alcohols and mixtures of hydrogen bonding solvents, L_{max} reflects the characteristic size of solvent domains that arises from intermolecular solvent structures.[14b] As the characteristic size of hydrogen-bonded domains is much larger than a single solvent molecule, the L_{max} values are considerably smaller in associative solvents compared with nonassociative solvents. The corresponding decrease in L_{max} indicates that the lower moments of the charge distribution play a more important role in determining the friction.[14b] However, there is no clear-cut way of finding out the value of L_{max} in the case of associative solvents, and thus, in practice, it has been used as an adjustable parameter in the AW analysis. Because the cavity radius is the property of the solute molecule, it should remain the same in associative and nonassociative solvents. Thus, the average value of the obtained cavity radii for acetone, DMF, and DMSO has been used in the analysis involving methanol and ethanol. A similar approach has been taken by Alavi et al. [14b] and Dutt et al.[72] The best fit L_{max} values for both methanol and ethanol equal 2. The agreements between the experimentally measured reorientation times of OX750 in methanol and ethanol and the theoretically calculated numbers are within 15% and 25%, respectively.

C. Biexponential Decays and the Fast Component. The biexponential anisotropy decay of medium probes, such as OX750, is more an exception than a rule, and there is little on this subject in the literature. As predicted by the SED theory, in the general case, only when a molecule possesses an axis of symmetry and the transition dipole is perpendicular to the symmetry axis, can the biexponential anisotropy decays be observed.[1] That is because, when the transition dipole is perpendicular to the symmetry axis, both tumbling and spinning will change the dipole orientation. OX750 is asymmetric and it does not possess an axis of symmetry. As discussed earlier, the transition dipole of OX750 between the ground state and first excited state is almost along with the long axis. In addition, the functional form of $r(t)$ predicted by the SED theory should be independent of solvent, contrary to what is observed experimentally. Thus, the SED theory cannot explain the departure from exponential kinetics observed here.

As mentioned earlier, our experiment results may indicate that the anisotropy decay laws of OX750 in alcoholic solvents are different from those in DMF and DMSO. Thus, this subsection will discuss two topics: the biexponential decays of OX750 in alcoholic solvents and the biexponential decays of OX750 in DMF and DMSO.

In Alcoholic Solvents. On the solvation dynamics of coumarin 153 (C153), Maroncelli and Fleming have observed a biexponential anisotropy of C153 in *n*-propanol and found a correlation between the fast rotational component and the solvation time.[73] Such behavior and correction also have been observed for 7-(diethylamino)-4-methylcoumarin (C1) in *n*-alcohols by Gustavsson et al.[74] In these studies, two possibilities for the origin of the fast component has been evoked. The first is that there is a substantial change in the dipole direction between S_0 and S_1. Then, immediately after absorption, an instantaneous torque on the S_1 dipole produced by the misaligned reaction field of the Franck−Condon solvent state will cause a forced rotation of solvent. This forced rotation could be considerably faster than diffusive rotation and account for the fast component. The ab initio calculations show that the dipole moment of OX750 on S_0 and S_1 are both located at the central ring of OX750 and that the directions are both from the N atom to O atom. Thus, this explanation can be ruled out on that basis. The second explanation involves the electronic charge redistribution in S_1, which is controlled by solvation, causing a rotation of the transition moment. In our previous experimental and theoretical studies of OX750 in *n*-alcohols,[56] the electron transfer (ET) reaction taking place from the alcoholic solvents to the OX750 chromophore was found. The intermolecular ET passing through the site-specific intermolecular hydrogen bonds exhibits unambiguous site selectivity. That is, the intermolecular ET can take place only in the intermolecular charge transfer (ICT) state passes through the hydrogen bond O−H···N, which is formed between the nitrogen atom in the central ring of OX750 and alcoholic solvents, and not by the stronger one of N−H···O, which is formed between the protonation site of OX750 and alcoholic solvents. Thus, the electronic charge of OX750 in the excited state will be redistributed as a result of the intermolecular ET reaction, causing a fast rotation of the transition moment. In addition, our previous theoretical results have shown that the hydrogen bond O−H···N is significantly strengthened in the excited state and that the hydrogen bond N−H···O is not influenced by photoexcitation.[56] The strengthening of the hydrogen bond may produce a torque and a rotation of the solute that is faster than the diffusion rotation.[74] According to the above discussions, we believe the most likely explanation is that the fast anisotropy decays observed in methanol and ethanol arise from the electronic coupling between the solute and solvent in the hydrogen-bonding site O−H···N.

Another possible explanation for the short component in the anisotropy decay may involve the effects of non-Markovian friction on the rotational motion, which has been used by Horng et al. to explain the nonexponential anisotropy decays of C153 in a number of solvents.[35] That is, in many solvents, the time-dependent friction on the rotational motion is not fast enough to lead to purely exponential rotational decays. Horng et al.[35] have studied the rotational dynamics of C153 in a great variety of solvents, finding that the anisotropy decays of C153 are

nonexponential even in some of the nonpolar solvents. Because fewer solvents were used in the present study, the anisotropy decay of OX750 in other solvents was not determined. Thus, this explanation could not be ruled out.

In DMF and DMSO. Unlike in methanol and ethanol, the nonexponential anisotropy decay of OX750 in DMF and DMSO can be seen clearly at first glance of the experimental data (see bottom panel of Figure 3.). The two processes of rotational relaxation in the anisotropy decays can be regarded as separate, and a two-step model should be used to explain such behavior. Moreover, the short component in the anisotropy decays is about hundreds of times faster than the time scale of the long component. This disparity in time scales suggests that the fast component could not be connected to the motion of the whole OX750 molecule, which may point to the ethyl group of OX750. A possible explanation for such biexponential anisotropy decays observed here is the extended wobbling-in-the-cone model.[75,76] According to this model, the faster rotational relaxation with a shorter correlation time is described as the motion of a restricted rotor, whereby the transition dipole moment can undergo orientational diffuse only within a cone of semiangle θ. The longer correlation time is accounted for as the slower overall orientational relaxation without any angular restriction. In this model, the anisotropy decay was fitted using the function[77]

$$r(t) = r(0)\, C_2(t) = r(0)[Q^2 + (1 - Q^2)\exp(-t/\tau_c)]\exp(-t/\tau_m) \quad (15)$$

where $r(0)$ is the initial anisotropy and Q^2 is the generalized order parameter that characterizes the cone semiangle in which fast orientational motion occurs. The time constants τ_c and τ_m are the time scales for orientational motion in the cone and slower diffusion motion, respectively. In our analysis, the experimentally measured anisotropy for OX750 in DMF and DMSO was fitted using the function

$$r(t) = r(0)[a\exp(-t/\tau_1) + (1 - a)\exp(-t/\tau_2)] \quad (16)$$

The obtained time constants τ_1 and τ_2 are presented in Table 2. Thus, τ_m is equal to τ_2, τ_c can be obtained using the relation

$$\tau_c = (\tau_1^{-1} - \tau_2^{-1})^{-1} \quad (17)$$

As the obtained τ_2 is about hundreds of times larger than τ_1, τ_c can be seen as equal to τ_1 according to eq 17. The cone semiangle θ can be obtained from the order parameter Q^2 using[75]

$$Q^2 = [{}^1/_2(\cos\theta)(1 + \cos\theta)]^2 \quad (18)$$

The values of Q^2 for DMF and DMSO from the fit are 0.837 and 0.832, respectively. The calculated cone semiangles for these two solvents are almost the same, about 20°. Thus, the anisotropy decays of OX750 in DMF and DMSO can be described as follows: First, the ethyl group of OX750 undergoes an ultrafast wobbling-in-the-cone orientational motion on the hundreds of femtoseconds time scale within a cone semiangle of 20°, and following, the OX750 molecules undergo diffusive orientational motion on the hundreds of picoseconds time scale.

Now, there are two questions that need to be addressed. First, what is the source of the restriction for such wobbling-in-the-cone orientational motion observed here for OX750? Second, why was such ultrafast restricted orientational motion observed only in DMF and DMSO? In response to the first question, we noticed that the restricted orientational motion of ethyl group may arise from the hydrogen bond that is formed between the solvent and the protonation site of OX750, because the associated solvent molecule is closer to the ethyl group. However, as mentioned earlier, all solvents used in the current work can form a hydrogen bond with the protonation site of OX750. Thus, the answer to the second question should be connected to the strength of this hydrogen bond in different solvents. That is, in DMF and DMSO, the strength of this hydrogen bond may be strong enough that the motion of the ethyl group is restricted in a cone by the associated solvent molecule. In other solvents, the strength of this hydrogen bond is not strong enough to cause a restricted motion of the ethyl group. To examine whether this idea seems reasonable, geometry optimizations have been performed for the ground-state of the solute−solvent complexes using the B3LYP/6-311+G** method, where the solvent molecule is associated with the protonation site of OX750. The calculated lengths of the hydrogen bond and hydrogen-bonding energies of the solute−solvent complexes are presented in Table 3. From Table 3 it can be seen that, in DMF and DMSO, the calculated lengths of the hydrogen bond are apparently shorter than those in other solvents used here. The calculated hydrogen-bonding energies for the OX750/DMF and OX750/DMSO complexes are also larger than others, indicating that the strength of the hydrogen bond in DMF and DMSO is actually greater than that in other solvents.

TABLE 3: Calculated Lengths of Hydrogen Bond (R) and Hydrogen-Bonding Energies (E_H) of Solute−Solvent Complexes Using Ab Initio Molecular Orbital Theory, Where the Solvent Was Associated with the Protonation Site of OX750

	R (Å)	E_H (kJ·mol^{-1})
OX750/acetone	2.081	39.752
OX750/methanol	2.078	33.748
OX750/ethanol	2.098	33.087
OX750/DMF	1.975	54.659
OX750/DMSO	1.914	60.392
OX750/formamide	2.033	47.846

D. In the Higher Excited State. With the pump pulse at 400 nm, the OX750 molecules will be excited from the ground state to a higher excited state (S_n). As mentioned earlier, the anisotropy decay of OX750 in this higher excited state is similar to that in the first excited state (see Table 2). The three classes of anisotropy decay laws for OX750 in S_1 also has been observed in this higher excited state. This confirms that the nonexponential anisotropy decays of OX750 in many solvents are not an artifact of the method of obtaining anisotropies but rather a reflection of some real physical processes. The representative time-resolved anisotropy decays of OX750 in acetone, ethanol, and DMF in this higher excited state are shown in Figure 7. From Figure 7 it can be seen that the initial values of anisotropy ($r(0)$) of OX750 in this higher excited state are apparently smaller than those in the first excited state. Irrespective of the solvents, we find that in this higher and the first excited state, the $r(0)$ values lie within the range 0.20−0.25 and 0.34−0.39, respectively. The lower initial values of anisotropy in this higher excited state mean a larger angle between the absorption and emission dipoles compared with the first excited state, according to the relation[3]

$$r(0) = \frac{2}{5}\left(\frac{3\cos^2\alpha - 1}{2}\right) \quad (19)$$

where α is the angle between the absorption and emission dipole moments of the probe. Because the parameters for a higher excited state required by the SED theory[1] and the AW

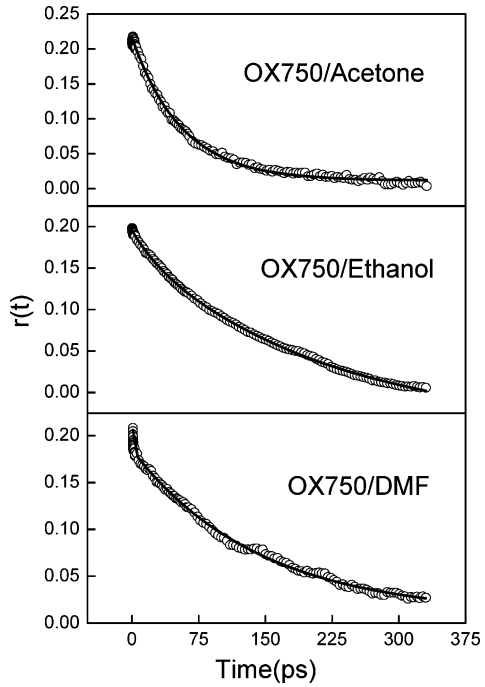

Figure 7. Anisotropy decays for oxazine 750 in acetone, ethanol and DMF on the pump pulse at 400 nm: (○) experimental data; (—) simulated results.

model,[46,47] such as charge distribution, were difficult to obtain accurately from the ab initio calculations, a quantitative analysis of the anisotropy decays for OX750 in this higher excited state was not presented here.

Conclusions

In summary, we have measured the anisotropy decays of OX750 in the first and a higher excited state in different solvents. In both excited states, three different anisotropy decay laws have been observed for OX750 in different solvents. As with most of the medium probes that have been studied in earlier publications, the exponential anisotropy decays have been found for OX750 in acetone and formamide and the obtained reorientation times have been ascribed to the overall rotational relaxation of the OX750 molecules. In the alcoholic solvents used here, methanol and ethanol, the faster anisotropy decay on the order of picoseconds and the slower anisotropy decay on the hundreds of picoseconds time scale are observed. The faster anisotropy decay may account for the rotation of the transition dipole moment in the excited state of OX750, which is caused by the electron transfer (ET) reaction taking place from the alcoholic solvents to the OX750 chromophore. In DMF and DSMO, the anisotropy decay of OX750 exhibits an apparent biexponential behavior and the obtained time constant for the fast component is on the order of hundreds of femtoseconds. As far as we know, the fast anisotropy decays on the order of hundreds of femtoseconds have not been reported for medium probes, such as OX750, in bulk solvents. As a possible explanation, the extended wobbling-in-the-cone model[75,76] has been employed to analyze the anisotropy decays of OX750 in DMF and DMSO. That is, the ethyl group of OX750 first undergoes an ultrafast wobbling-in-the-cone orientational motion on the hundreds of femtosecond time scale within a cone semiangle of 20°, followed by the OX750 molecules undergoing diffusive orientational motion on the hundreds of picoseconds time scale. According to our theoretical studies, the wobbling-in-the-cone motion of the ethyl group of OX750 may occur only when the hydrogen bond formed between the solvent and the protonation site of OX750 is strong enough, as is the case with DMF and DMSO. Using the SED theory[1] and AW model,[46, 47] a quantitative analysis of the long time anisotropy decays observed in all of the solvents has been carried out. Our analysis has shown that the experimental results can be reproduced by using the SED theory with the slip boundary condition combined with the AW model. Although the cavity radius of the solute molecule or L_{max} is used as an adjustable parameter in the AW model, the best fit cavity radius of OX750 in aprotic solvents is closer to the long axial radius of OX750, which is satisfied with the criterion of the AW model,[71] indicating that a reasonable agreement between the experiment and theory has been achieved. The anisotropy decays of OX750 in the two excited states investigated here are almost the same, with the exception that the $r(0)$ values in the higher excited state are lower than those in the first excited state. This may indicate that the anisotropy decay laws observed here for OX750 are not state-dependent.

Our experiment results have demonstrated that, even in bulk solvents, the fast anisotropy decays on the femtosecond time scale are present for the medium probes, such as OX750, and may play an important role in understanding the fundamental nature of solvent−solute interactions. More theoretical and experimental studies of the anisotropy decays on femtosecond time scale are deserved.

Acknowledgment. This work is supported by the National Natural Science Foundation of China (Grant 20403020 and 20633070), the Knowledge Innovation Program of the Chinese Academy of Sciences (Grant DICP K2007/F2), and NKBRSF (Grant 2007CB815202).

References and Notes

(1) Fleming, G. R. *Chemical Applications of Ultrafast Spectroscopy*; Oxford University Press: New York, 1986.
(2) Lakowicz, J. R. *Principles of Fluorescence Spectroscopy*; Plenum Press: New York and London, 1983.
(3) Dutt, G. B. *Chem. Phys. Chem.* **2005**, *6*, 413.
(4) Lettenberger, M.; Emmerling, F.; Gottfried, N. H.; Laubereau, A. *Chem. Phys. Lett.* **1995**, *240*, 324.
(5) Emmerling, F.; Lettenberger, M.; Laubereau, A. *J. Phys. Chem.* **1996**, *100*, 19251.
(6) Barbour, L. W.; Hegadorn, M.; Asbury, J. B. *J. Phys. Chem. B* **2006**, *110*, 24281.
(7) Gaab, K. M.; Bardeen, C. J. *Phys. Rev. Lett.* **2004**, *93*, 056001.
(8) Fleming, G. R.; Knight, A. E. W.; Morris, J. M.; Robbins, R. J.; Robinson, G. W. *Chem. Phys. Lett.* **1977**, *49*, 1.
(9) Hyde, P. D.; Ediger, M. D. *J. Chem. Phys.* **1990**, *92*, 1036.
(10) Kim, Y. P.; Hochstrasser, R. M. *J. Phys. Chem.* **1992**, *96*, 9595.
(11) Blanchard, G. J.; Cihal, C. A. *J. Phys. Chem.* **1988**, *92*, 5950.
(12) de Bekker, E. J.; Pugzlys, A.; Varma, C. A. G. O. *J. Phys. Chem. A* **2002**, *106*, 5974.
(13) Alavi, D. S.; Hartman, R. S.; Waldeck, D. H. *J. Chem. Phys.* **1991**, *94*, 4509.
(14) (a) Alavi, D. S.; Hartman, R. S.; Waldeck, D. H. *J. Chem. Phys.* **1991**, *95*, 6770. (b) Hartman, R. S.; Alavi, D. S.; Waldeck, D. H. *Isr. J. Chem.* **1993**, *33*, 157.
(15) Alavi, D. S.; Waldeck, D. H. *J. Phys. Chem.* **1991**, *95*, 4848.
(16) Hartman, R. S.; Alavi, D. S.; Waldeck, D. H. *J. Phys. Chem.* **1991**, *95*, 7872.
(17) Hartman, R. S.; Konitsky, W. M.; Waldeck, D. H. *J. Am. Chem. Soc.* **1993**, *115*, 9692.
(18) Balabai, N.; Waldeck, D. H. J. *Phys. Chem. B* **1997**, *101*, 2339.
(19) Balabai, N.; Kurnikova, M. G.; Coalson, R. D.; Waldeck, D. H. *J. Am. Chem. Soc.* **1998**, *120*, 7944.
(20) Dutt, G. B.; Singh, M. K.; Sapre, A. V. *J. Chem. Phys.* **1998**, *109*, 5994.
(21) Dutt, G. B.; Srivatsavoy, V. J. P.; Sapre, A. V. *J. Chem. Phys.* **1999**, *111*, 9705.
(22) Dutt, G. B.; Ghanty, T. K. *J. Phys. Chem. B* **2003**, *107*, 3257.
(23) Dutt, G. B.; Srivatsavoy, V. J. P.; Spare, A. V. *J. Chem. Phys.* **1999**, *110*, 9623.

(24) Dutt, G. B.; Ghanty, T. K. *J. Chem. Phys.* **2004**, *121*, 3625.
(25) Dutt, G. B.; Ghanty, T. K. *J. Phys. Chem. A* **2004**, *108*, 6090.
(26) Dutt, G. B.; Raman, S. *J. Chem. Phys.* **2001**, *114*, 6702.
(27) Dutt, G. B.; Krishna, G. R.; Raman, S. *J. Chem. Phys.* **2001**, *115*, 4732.
(28) Dutt, G. B.; Ghanty, T. K.; Singh, M. K. *J. Chem. Phys.* **2001**, *115*, 10845.
(29) Kim, S. K.; Fleming, G. R. *J. Phys. Chem.* **1988**, *92*, 2168.
(30) Dutt, G. B.; Krishna, G. R. *J. Chem. Phys.* **2000**, *112*, 4676.
(31) Tao, T. *Biopolymers* **1969**, *8*, 609.
(32) Chuang, T. J.; Eisenthal, K. B.; *J. Chem. Phys.* **1972**, *57*, 5094.
(33) Jas, G. S.; Wang, Y.; Pauls, S. W.; Johnson, C. K.; Kuczera, K. *J. Chem. Phys.* **1997**, *107*, 8800.
(34) Brocklehurst, B.; Young, R. N. *J. Phys. Chem. A* **1999**, *103*, 3809.
(35) Horng, M. L.; Gardecki, J. A.; Maroncelli, M. *J. Phys. Chem.* **1997**, *101*, 1030.
(36) Sukharevsky, A. P.; Read, I.; Linton, B.; Hamilton, A. D.; Waldeck, D. H. *J. Phys. Chem. B* **1998**, *102*, 5394.
(37) Zhong, Q.; Wang, Z.; Sun, Y.; Zhu, Q.; Kong, F. *Chem. Phys. Lett.* **1996**, *248*, 277.
(38) Zhong, Q.; Wang, Z.; Liu, Y.; Zhu, Q.; Kong, F. *J. Chem. Phys.* **1996**, *105*, 5377.
(39) He, Y.; Xiong, Y.; Wang, Z.; Zhu, Q.; Kong, F. *J. Phys. Chem. A* **1998**, *102*, 4266.
(40) Liu, J. Y.; Fan, W. H.; Han, K. L.; Xu, D. L.; Lou, N. Q. *J. Phys. Chem. A* **2003**, *107*, 1914.
(41) Liu, J. Y.; Fan, W. H.; Han, K. L.; Deng, W. Q.; Xu, D. L.; Lou, N. Q. *J. Phys. Chem. A* **2003**, *107*, 10857.
(42) Shi, Y.; Liu, J. Y.; Han, K. L. *Chem. Phys. Lett.* **2005**, *410*, 260.
(43) Zhou, L. C.; Liu, J. Y.; Zhao, G. J.; Shi, Y.; Peng, X. J.; Han, K. L. *Chem. Phys.* **2007**, *333*, 179.
(44) Guo, X.; Wang, S.; Xia, A.; Su, H. *J. Phys. Chem. A* **2007**, *111*, 5800.
(45) Gong, Y.; Guo, X.; Wang, S.; Su, H.; Xia, A.; He, Q.; Bai, F. *J. Phys. Chem. A* **2007**, *111*, 5806.
(46) Alavi, D. S.; Waldeck, D. H. *J. Chem. Phys.* **1991**, *94*, 6196.
(47) Alavi, D. S.; Waldeck, D. H. *J. Chem. Phys.* **1993**, *98*, 3580.
(48) Lee, C.; Yang, W.; Parr, R. G. *Phys. Rev. B* **1988**, *37*, 785.
(49) Becke, A. D. *J. Chem. Phys.* **1993**, *98*, 5648.
(50) Stephens, P. J.; Devlin. F. J.; Chabalowski, C. F.; Frisch, M. J. *J. Phys. Chem.* **1994**, *98*, 11623.
(51) Frisch, M. J.; Trucks, G. W.; Schlegel, H. B.; Scuseria, G. E.; Robb, M. A.; Cheeseman, J. R.; Montgomery, J. A., Jr.; Verven, T.; Kudin, K. N.; Burant, J. C.; Millam, J. M.; Iyengar, S. S.; Tomasi, J.; Barone, V.; Mennucci, B.; Cossi, M.; Scalmani, G.; Rega, N.; Petersson, G. A.; Nakatsuji, H.; Hada, M.; Ehara, M.; Toyota, K.; Fukuda, R.; Hasegawa, J.; Ishida, M.; Nakajima, T.; Honda, Y.; Kitao, O.; Nakai, H.; Klene, M.; Li, X.; Knox, J. E.; Hratchian, H. P.; Cross, J. B.; Adamo, C.; Jaramillo, J.; Gomperts, R.; Stratmann, R. E.; Yazyev, O.; Austin, A. J.; Cammi, R.; Pomelli, C.; Ochterski, J. W.; Ayala, P. Y.; Morokuma, K.; Voth, G. A.; Salvador, P.; Dannenberg, J. J.; Zakrzewski, V. G.; Dapprich, S.; Daniels, A. D.; Strain, M. C.; Farkas, O.; Malick, D. K.; Rabuck, A. D.; Raghavachari, K.; Foresman, J. B.; Ortiz, J. V.; Cui, Q.; Baboul, A. G.; Clifford, S.; Cioslowski, J.; Stefanov, B. B.; Liu, G.; Liashenko, A.; Piskorz, P.; Komaromi, I.; Martin, R. L.; Fox, D. J.; Keith, T.; Al-Laham, M. A.; Peng, C. Y.; Nanayakkara, A.; Challacombe, M.; Gill, P. M. W.; Johnson, B.; Chen, W.; Wong, M. W.; Gonzalez, C.; Pople, J. A. *Gaussian 03*, revision C.02; Gaussian, Inc.: Pittsburgh, PA, 2003.
(52) Horng, M. L.; Gardecki, J. A.; Papazyan, A.; Maroncelli, M. *J. Phys. Chem.* **1995**, *99*, 17311.
(53) Kubinyi, M.; Grofcsik, A.; Kárpáti, T.; Jones, W. J. *Chem. Phys.* **2006**, *322*, 247.
(54) Dutt, G. B.; Doraiswamy, S.; Periasamy, N.; Venkataraman, B. *J. Chem. Phys.* **1990**, *93*, 8498.
(55) (a) Imasaka, T.; Tsukamoto, A.; Ishibashi, N. *Anal. Chem.* **1989**, *61*, 2285. (b) Ghanadzadeh, A.; Tajalli, H.; Zirack, P.; Shirdel, J. *Spectrochim. Acta A* **2004**, *60*, 2925.
(56) Zhao, G. J.; Liu, J. Y.; Zhou, L. C.; Han, K. L. *J. Phys. Chem. B* **2007**, *111*, 8940.
(57) Hartman, R. S.; Waldeck, D. H. *J. Phys. Chem.* **1994**, *98*, 1386.
(58) Hubbard, J. B.; Onsager, L. *J. Chem. Phys.* **1977**, *67*, 4850.
(59) Hubbard, J. B. *J. Chem. Phys.* **1978**, *69*, 1007.
(60) Kurnikova, M. G.; Waldeck, D. H.; Coalson, R. D. *J. Chem. Phys.* **1996**, *105*, 628.
(61) Kumar, P. V.; Maroncelli, M. *J. Chem. Phys.* **2000**, *112*, 5370.
(62) Balabai, N.; Sukharevsky, A.; Read, I.; Strazisar, B.; Kurnikova, M.; Hartman, R. S.; Coalson, R. D.; Waldeck, D. H. *J. Mol. Liq.* **1998**, *77*, 37.
(63) Edward, J. T. *J. Chem. Educ.* **1970**, *47*, 261.
(64) (a) Youngren, G. K.; Acrivos, A. *J. Chem. Phys.* **1975**, *63*, 3846. (b) Sension, R. J.; Hochstrasser, R. M. *J. Chem. Phys.* **1993**, *98*, 2490.
(65) Small, E. W.; Isenberg, I. *Biopolymers* **1977**, *16*, 1907.
(66) Williams, A. M.; Jiang, Y.; Ben-Amotz, D. *Chem. Phys.* **1994**, *180*, 119.
(67) Kubinyi, M.; Grofcsik, A.; Pápai, I.; Jones, W. J. *Chem. Phys.* **2003**, *286*, 81.
(68) Kurnikova, M. G.; Balabai, N.; Waldeck, D. H.; Coalson, R. D. *J. Am. Chem. Soc.* **1998**, *120*, 6121.
(69) Van der Zwan, G.; Hynes, J. T. *J. Phys. Chem.* **1985**, *89*, 4181.
(70) Nee, T. W.; Zwanzig, R. *J. Chem. Phys.* **1970**, *52*, 6353.
(71) Hartman, R. S.; Konitsky, W. M.; Waldeck, D. H.; Chang, Y. J.; Castner, E. W., Jr. *J. Chem. Phys.* **1997**, *106*, 7920.
(72) Dutt, G. B.; Ghanty, T. K. *J. Chem. Phys.* **2003**, *118*, 4127.
(73) Maroncelli, M.; Flemimg, G. R. *J. Chem. Phys.* **1987**, *86*, 6221.
(74) Gustavsson, T.; Cassara, L.; Marguet, S.; Gurzadyan, G.; van der Meulen, P.; Pommeret, S.; Mialocq, J.-C. *Photochem. Photobiol. Sci.* **2003**, *2*, 329.
(75) Lipari, G.; Szabo, A. *Biophys. J.* **1980**, *30*, 489.
(76) Wang, C. C.; Pecora, R. *J. Chem. Phys.* **1980**, *72*, 5333.
(77) Tan, H.-S.; Piletic, I. R.; Fayer, M. D. *J. Chem. Phys.* **2005**, *122*, 174501.